FROM THEORY TO OBSERVATION

- **Masses are not directly observable. Galaxy clusters are selected according to some observable, in general related to the observational technique, which correlate with the mass.**

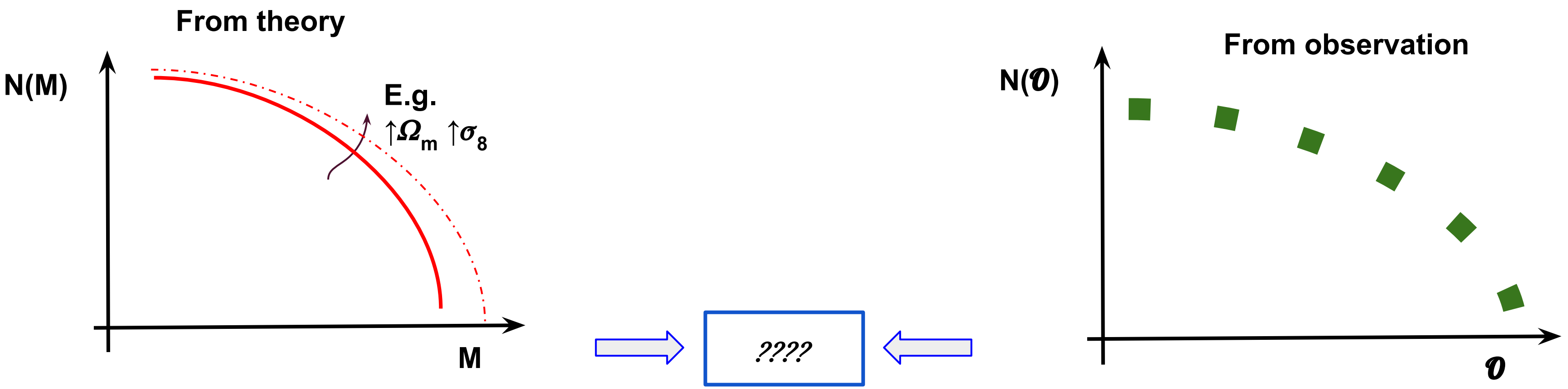

$\mathcal{O}$: Observable used to detect/select clusters (e.g. number of galaxies, X-ray luminosity, SZ signal)

FROM THEORY TO OBSERVATION

- **Individual mass measurements are expensive and not feasible for cluster survey. We need to rely on mass proxies which are tightly correlated with the halo mass.**

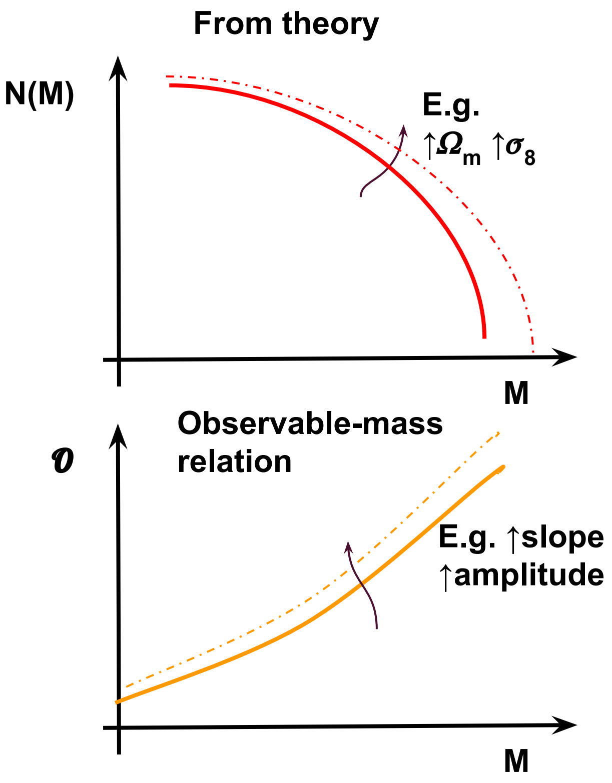

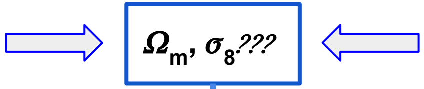

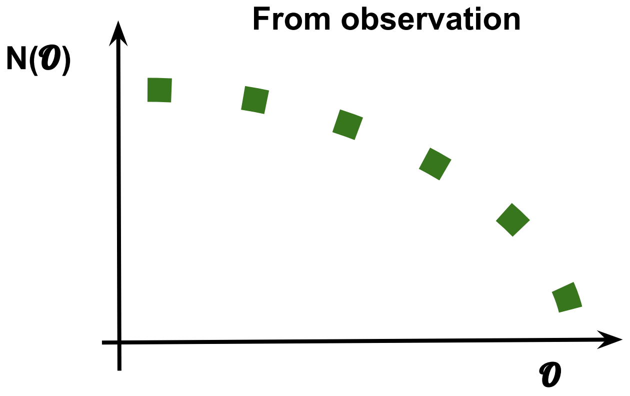

Cosmological and scaling relation parameters are in general highly degenerate, and follow-up data are necessary to constrain simultaneously cosmology and the observable-mass relation

LIMITATIONS FOR CLUSTER COSMOLOGY STUDIES

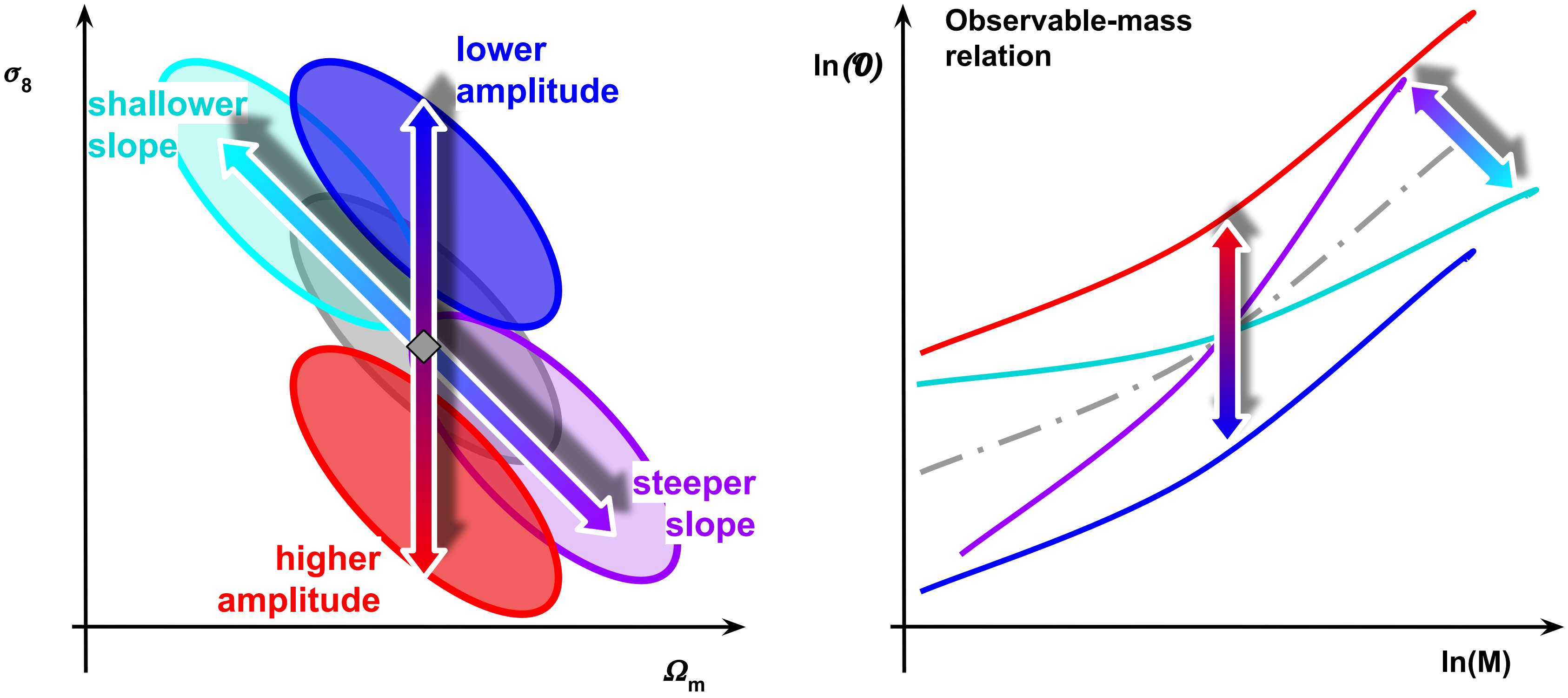

FROM THEORY TO OBSERVATION: CONSTRAINTS

- **Combine cluster abundance and cluster mass estimates data to simultaneously constrain cosmology and the observable-mass relation(s)**

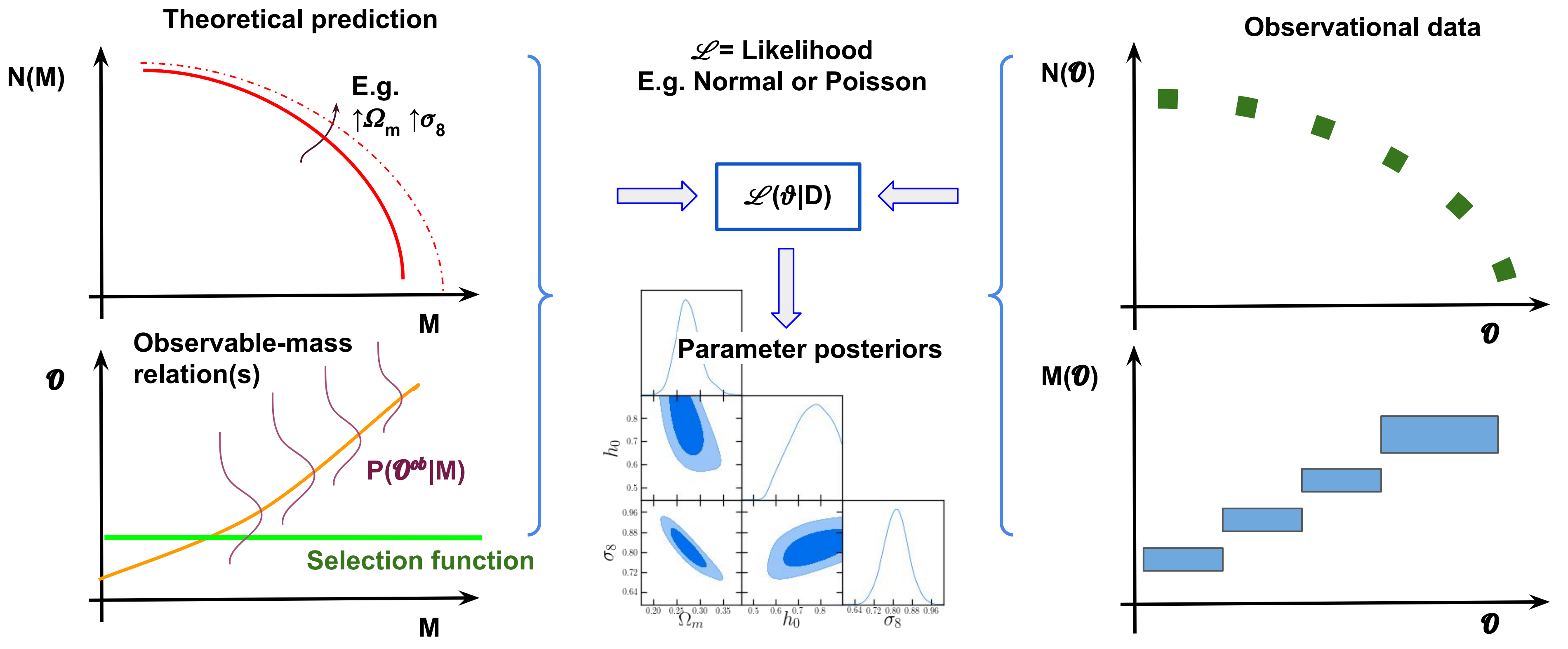

CLUSTER DETECTION: PHOTOMETRIC SURVEY

- **Detection:**
  - Overdensity of (red-sequence) galaxies
  - Lensing effect

- **Observable/Mass proxy:**
  - Richness (# member galaxies)
  - Luminosity
  - Lensing signal
  - Velocity dispersion (with spectra)

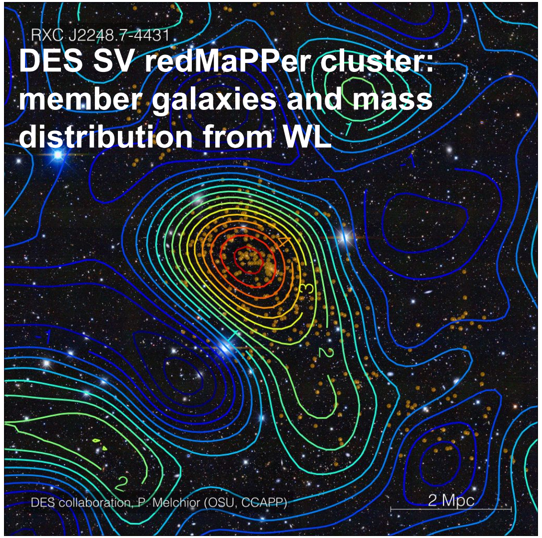

z-λ distribution of redMaPPer clusters in DES Y1

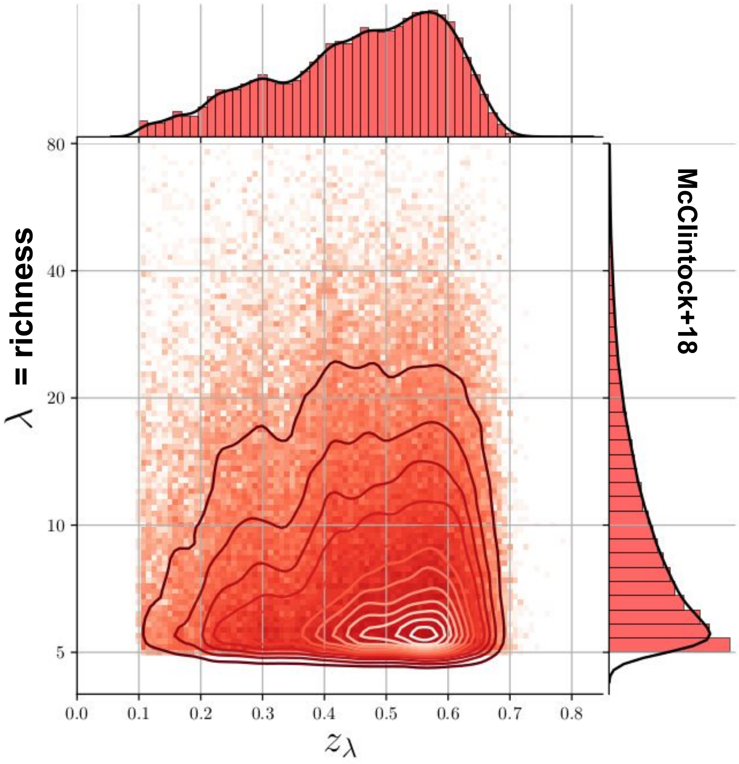

CLUSTER DETECTION: X-RAY SURVEY

- **Detection:**
  - **Extended x-ray sources**
- **Observable/Mass proxy:**
  - L_X
  - T_X
  - **Flux**
  - $Y_x = M_{gas}\, T_X$ **(gas thermal energy)**

X-ray images of clusters from eROSITA

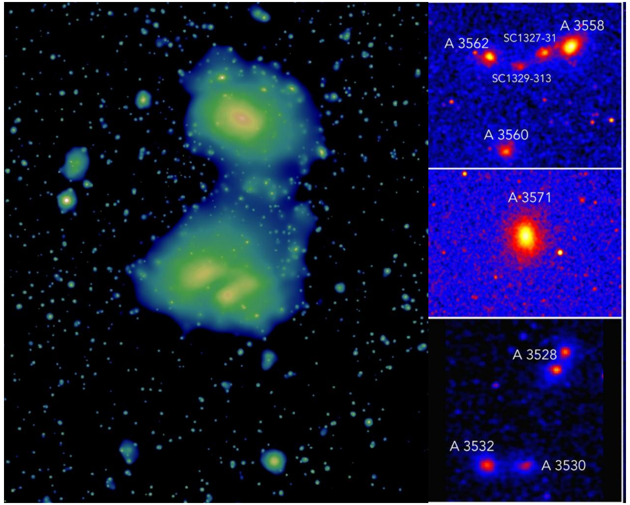

L_X, z distribution of X-ray selected catalogs

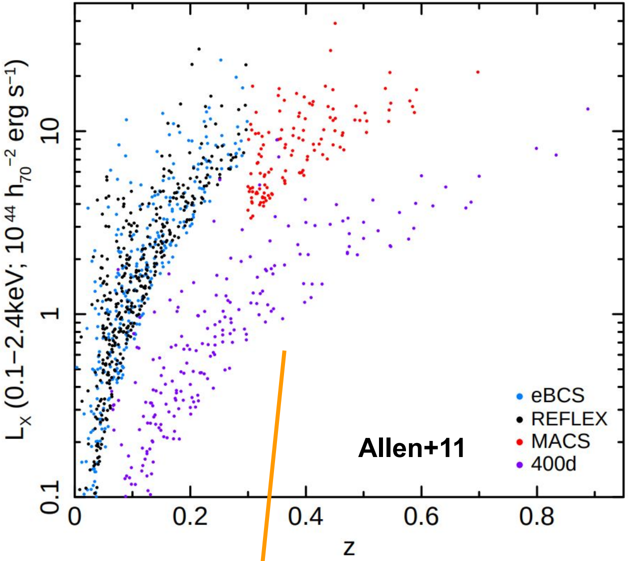

Flux limited sample

- **X-ray emissivity from *bremsstrahlung* radiation of the ICM:**

$$\epsilon_\nu \equiv \frac{dL}{dV d\nu} \propto n_e^2 g(\nu, T) T^{-1/2} \exp(-h\nu / k_B T)$$

Not very sensitive to projections

CLUSTER DETECTION: SZ SURVEY

- **Detection:**
  Thermal Sunyaev-Zel'dovich effect
  (mm-wavelength)

- **Observable/Mass proxy:**
  SZ signal

Mass and redshift distribution of SZ-selected cluster catalogs (Bleem+19)

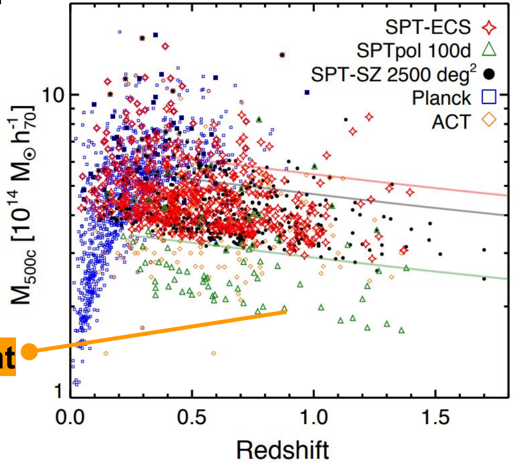

~ redshift independent

Thermal Sunyaev-Zel'dovich effect

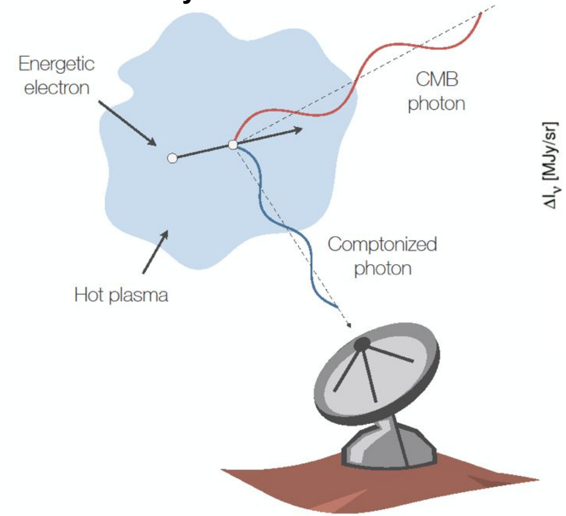

SZ spectral distortion

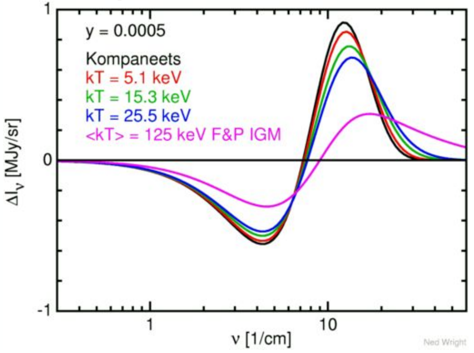

Compton-y parameter

$$y = \int \mathrm{d}l \frac{k_B T_e}{m_e c^2} n_e \sigma_\mathrm{T}$$

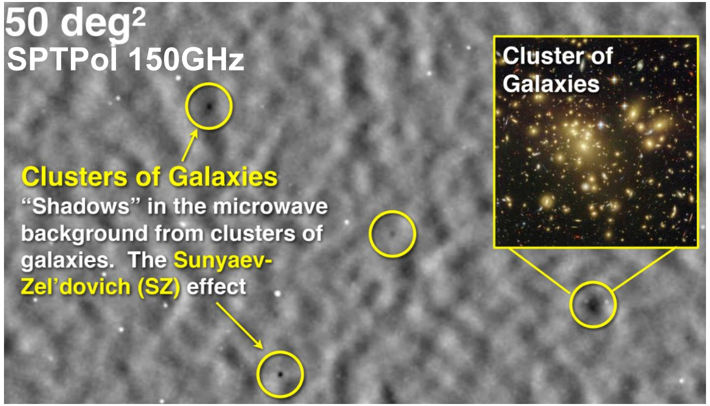

Credits B. Benson, SPT Collaboration

CLUSTER CATALOGS

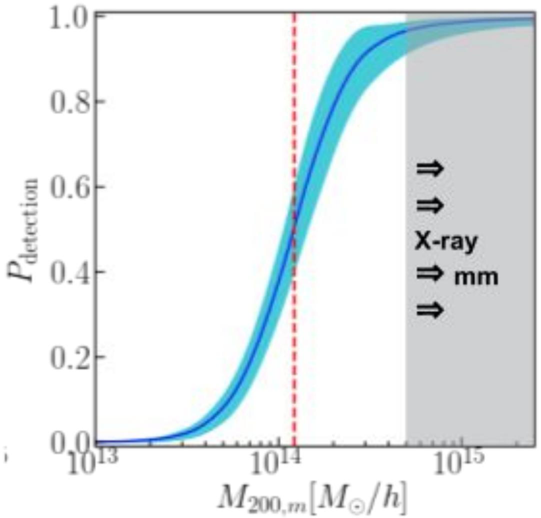

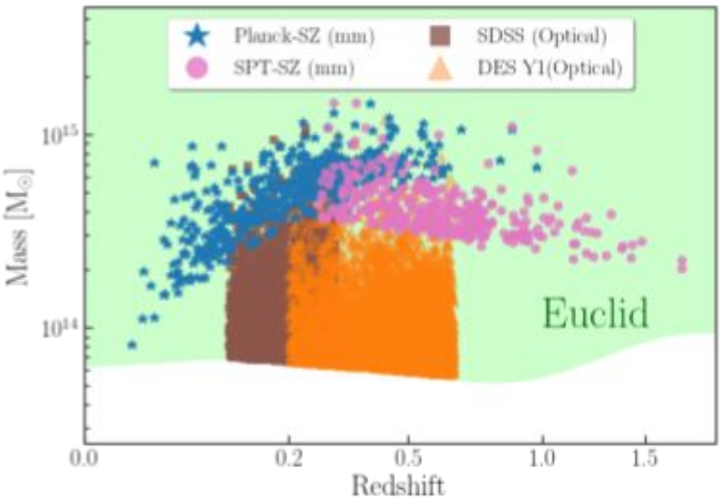

Figure 1: *Left*: redMaPPer DES Y1 cluster catalog detection probability as a function of mass: systems down to ~$5 \cdot 10^{13}$ $M_\odot$ have a non-negligible chance to be included in the optical catalog (λ>20), while clusters selected at different wavelength (X-ray, mm) have masses typically above $5 \cdot 10^{14}$ $M_\odot$ (*gray* area; adapted from [Ab20]). *Right*: Mass and redshift ranges probed by current optical (SDSS, DES Y1) and millimeter (Planck-SZ, SPT-SZ 2500) cluster surveys. The green shaded area marks the mass and redshift range to be covered by the Euclid cluster sample.

Photometric catalogs capable of detecting system down to group mass scale but have a much less cleaner selection function which hamper they cosmological exploitation

MASS MEASUREMENTS FROM X-ray DATA

- **From hydrostatic equilibrium:**

$$M(<r) = -\frac{r}{G}\frac{k_B T(r)}{\mu m_p}\left(\frac{\mathrm{d}\ln\rho_{\mathrm{gas}}(r)}{\mathrm{d}\ln r} + \frac{\mathrm{d}\ln T(r)}{\mathrm{d}\ln r}\right)$$

Assumptions:

- **Hydrostatic equilibrium (Negligible non-thermal pressure support)**
- **Spherical symmetry**

Temperature profiles from *XMM-Newton* observations (Pratt+06)

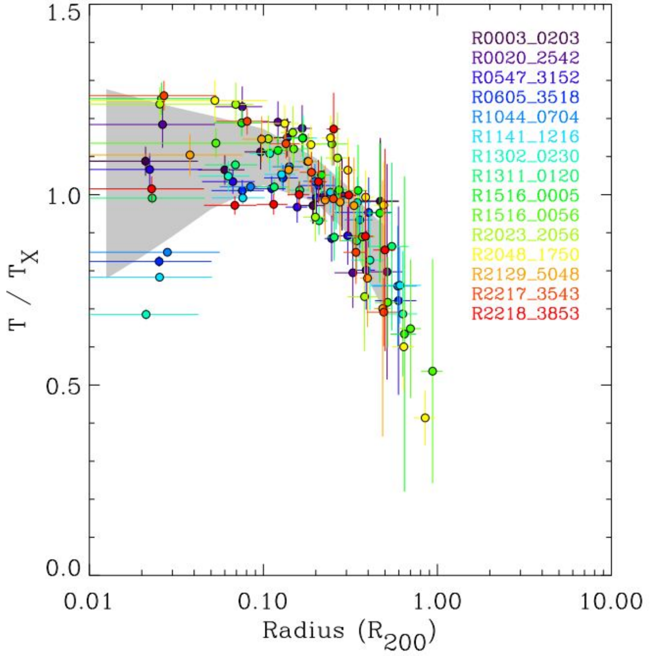

MASS MEASUREMENTS FROM SPECTROSCOPIC DATA

- **Dynamical mass estimates (Jeans equation):**

$$M(<r) = -\frac{r\sigma_r^2}{G}\left(\frac{d\ln\sigma_r^2}{d\ln r} + \frac{d\ln n_{glx}}{d\ln r} + 2\beta\right)$$

Assumptions:
- **Spherical symmetry**
- **Dynamical equilibrium**

L.o.s. velocity dispersion and member galaxy density profiles from VLT/VIMOS (Biviano+13)

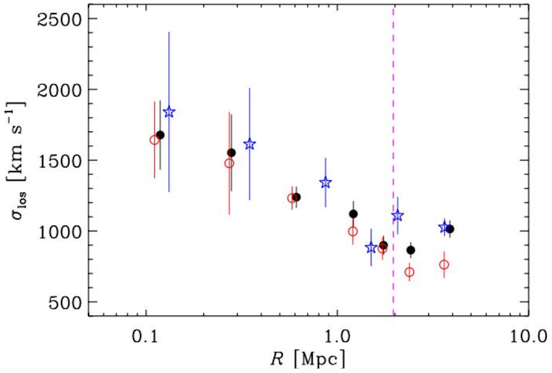

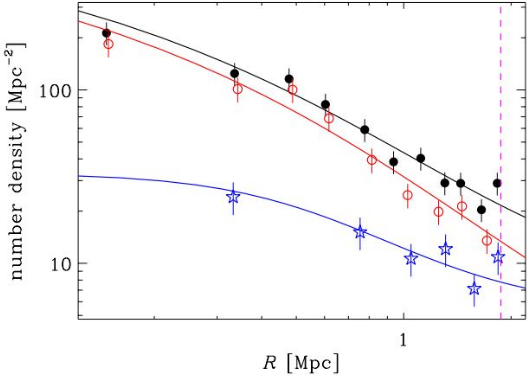

- **Caustic method (projected phase-space distribution):**

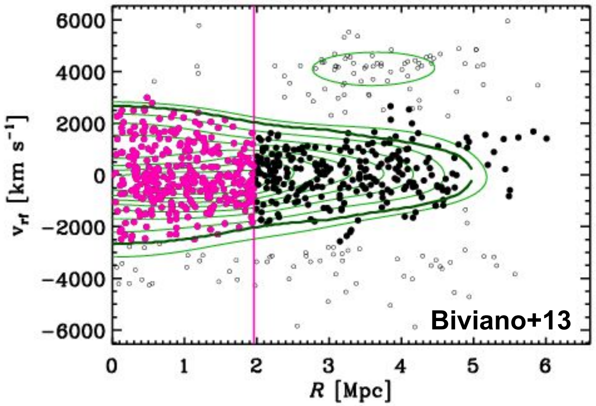

MASS MEASUREMENTS FROM IMAGING

- **Strong and Weak Lensing mass measurements:**

Projected density profile from strong lensing

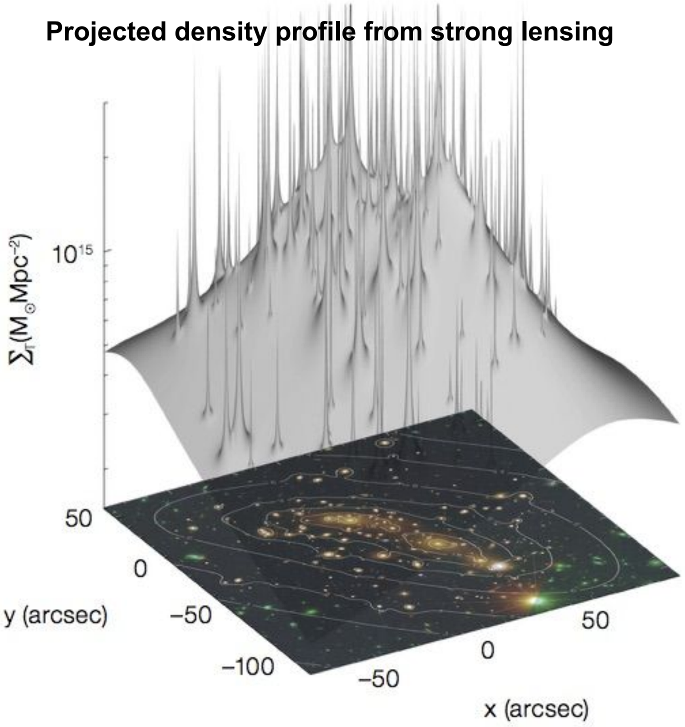

Tangential shear profile from WL (Dietrich+18)

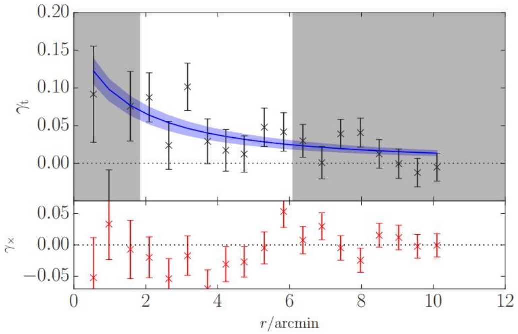

Cluster mass profile from different techniques (Battaglia+16)

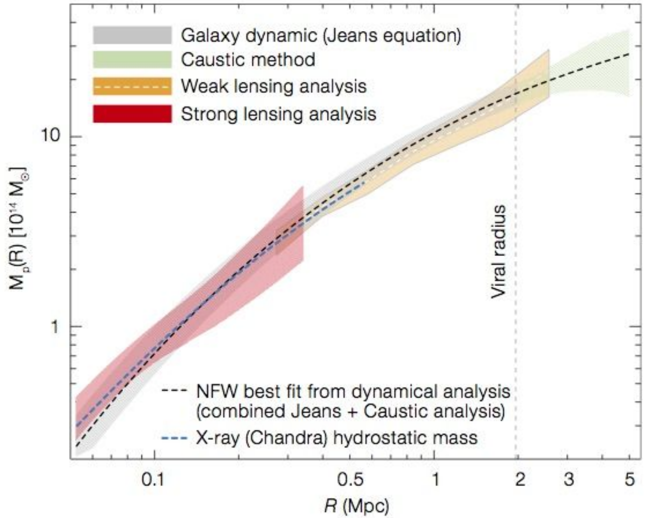

$$\gamma_t(n_s(z), \Sigma(R)) \Rightarrow \Sigma(R) = \int_{-\infty}^{\infty} d\,\chi\, \Delta\rho\left(\sqrt{R^2 + \chi^2}\right)$$

Assumption:

- **Parametric form for the halo density profile (e.g. NFW, Einasto profiles; Navarro+97, Einasto 1965) and correlated structures (2-halo term)**

CMB CLUSTER LENSING

- **Lensing by GC induces a dipole-like distortion in the CMB:**

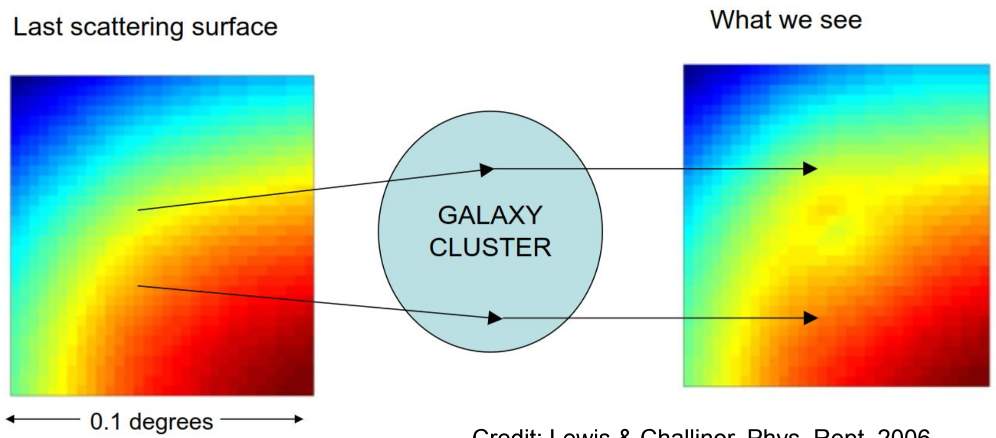

Credit: Lewis & Challinor, Phys. Rept. 2006

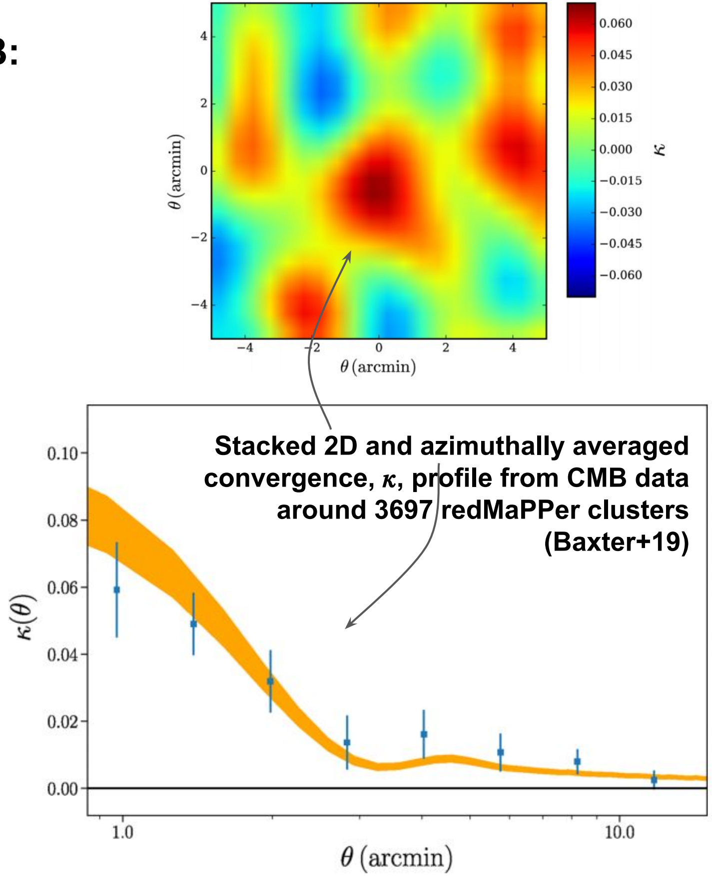

Stacked 2D and azimuthally averaged convergence, κ, profile from CMB data around 3697 redMaPPer clusters (Baxter+19)

The distortion is quite small (~10μK for $10^{15}M_\odot$ halo) but can be used to calibrate the mass of high redshift clusters.

The lensing signal can also be detected in polarization data (see e.g. Raghunathan+19).

FROM THEORY TO OBSERVATION: SCALING RELATIONS

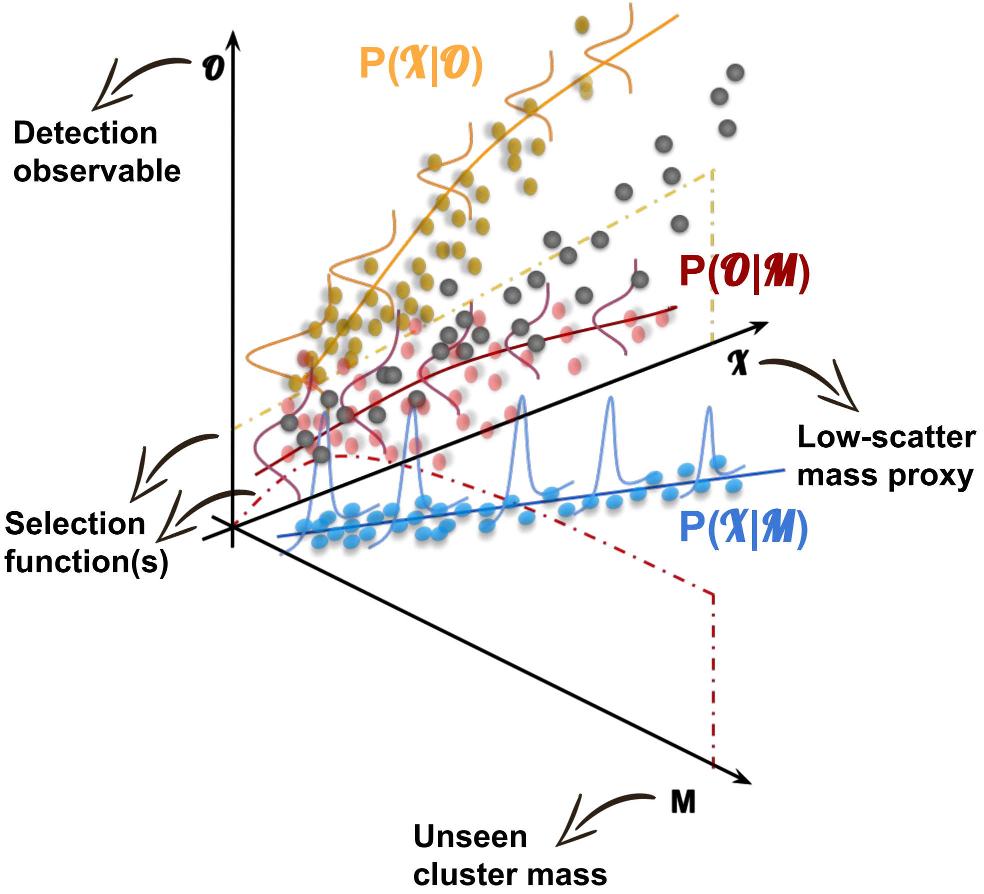

Different detection techniques imply different mass proxies, mass calibration data and systematics.

The calibration of the observable-mass relation(s) requires:

- **Well defined selection function(s)**
- **A model to describe the parent distribution as a function of mass (halo mass function)**
- **A model to describe the PDF of the multivariate observable space: P($\mathcal{X}$,$\mathcal{O}$|$\mathcal{M}$)**

FROM THEORY TO OBSERVATION: SCALING RELATIONS

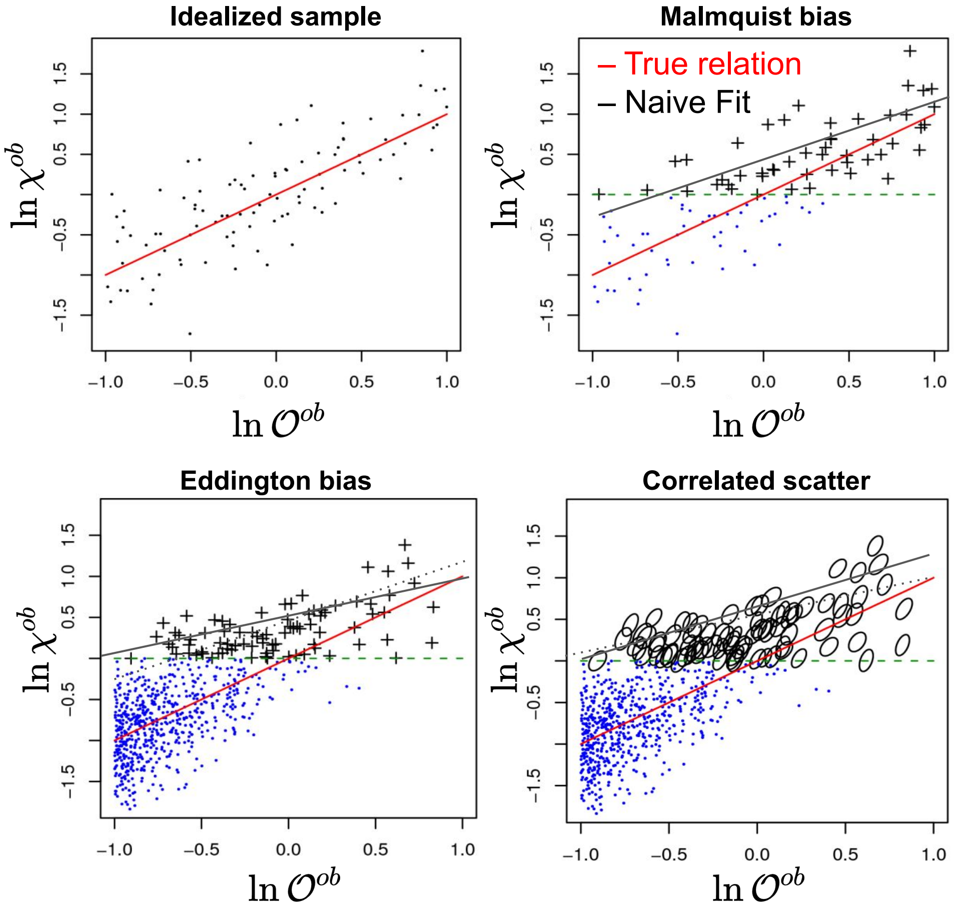

Credit A. Mantz

Different detection techniques imply different mass proxies, mass calibration data and systematics.

The calibration of the observable-mass relation(s) requires:

- **Well defined selection function(s)**
- **A model to describe the parent distribution as a function of mass (halo mass function)**
- **A model to describe the PDF of the multivariate observable space: $P(\mathcal{X},\mathcal{O}|\mathcal{M})$**

RECENT CONSTRAINTS FROM CLUSTER NC

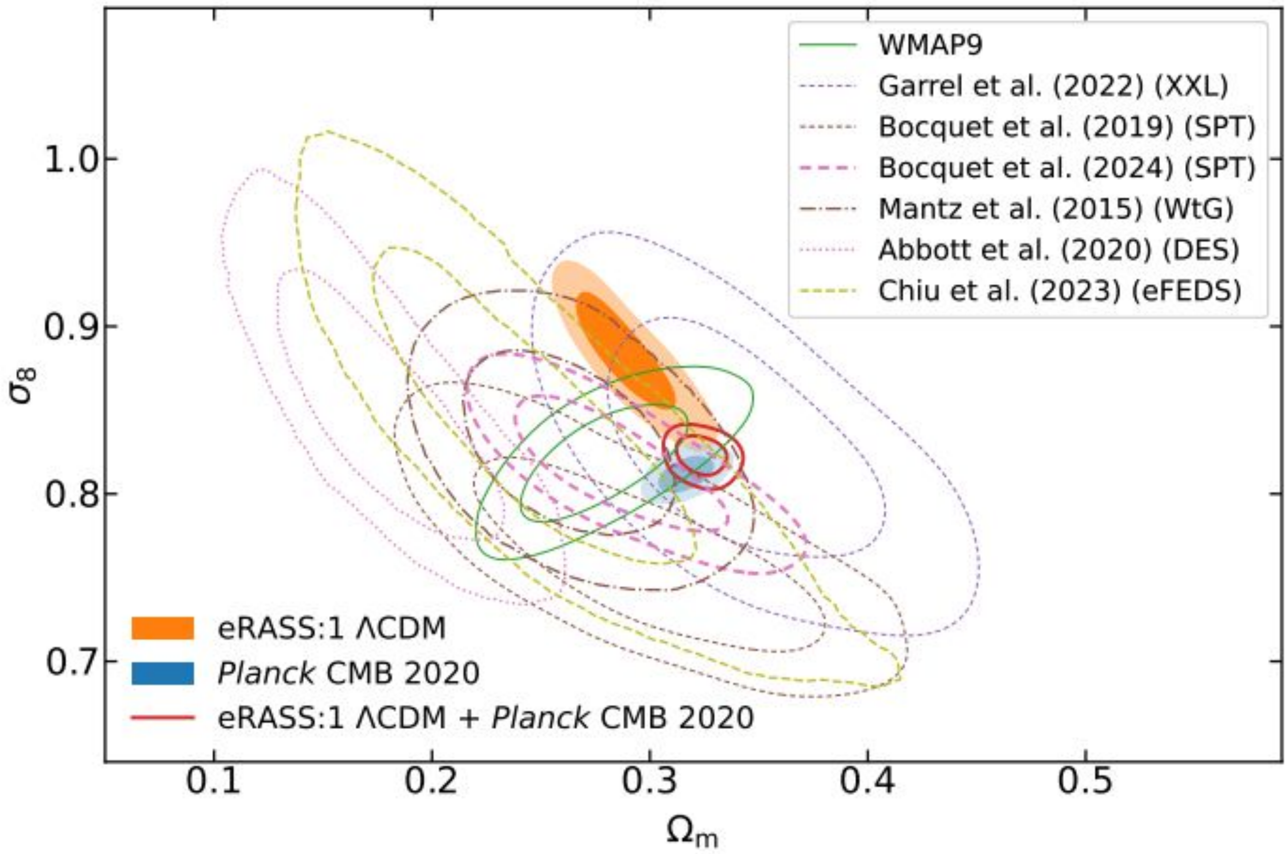

eRASS1:

$$\Omega_\mathrm{m} = 0.29^{+0.01}_{-0.02},$$
$$\sigma_8 = 0.88 \pm 0.02,$$
$$S_8 = 0.86 \pm 0.01.$$

https://arxiv.org/pdf/2402.08458.pdf

RECENT CONSTRAINTS FROM CLUSTER NC

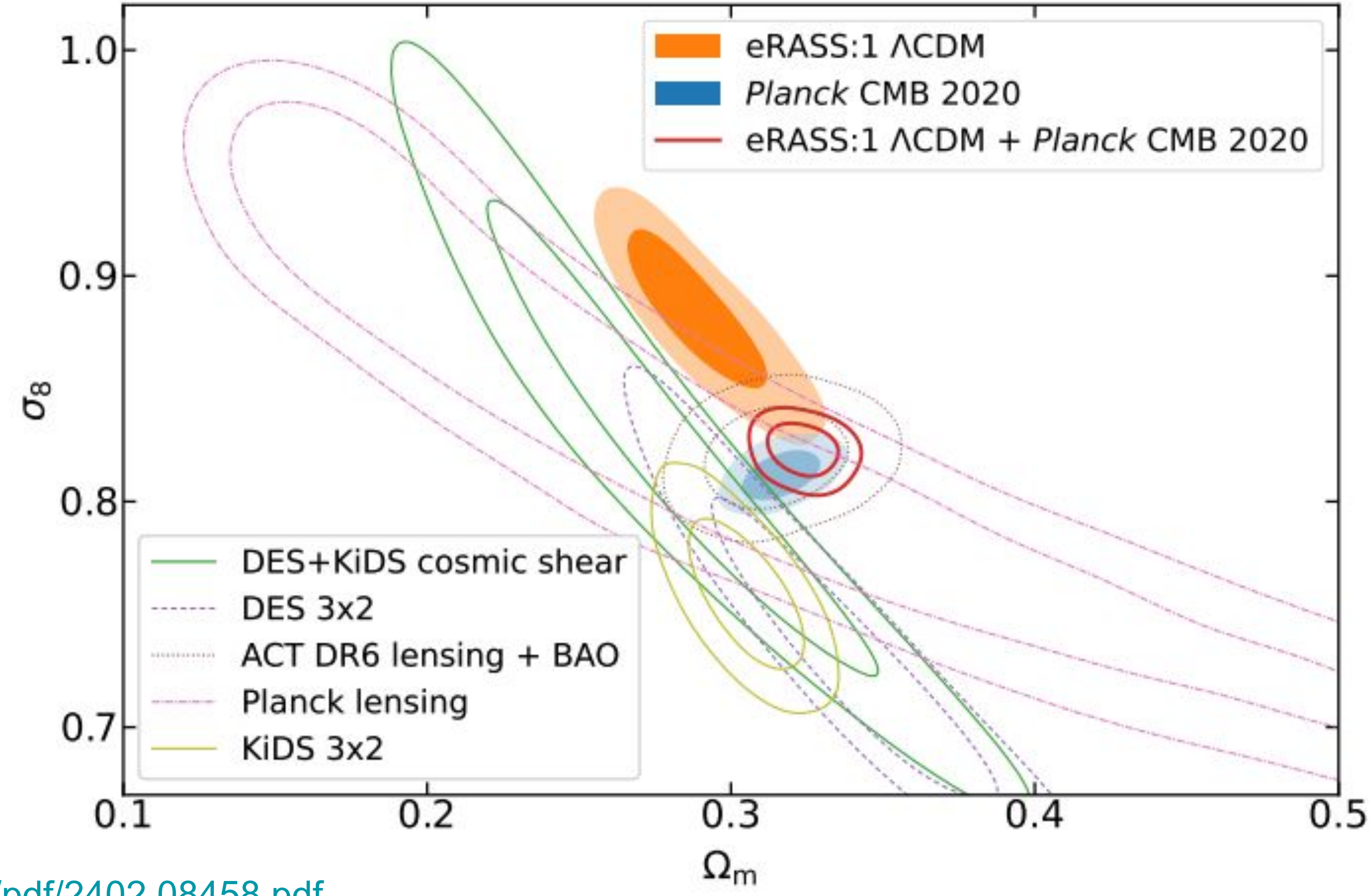

https://arxiv.org/pdf/2402.08458.pdf

LIMITATIONS FOR CLUSTER COSMOLOGY STUDIES

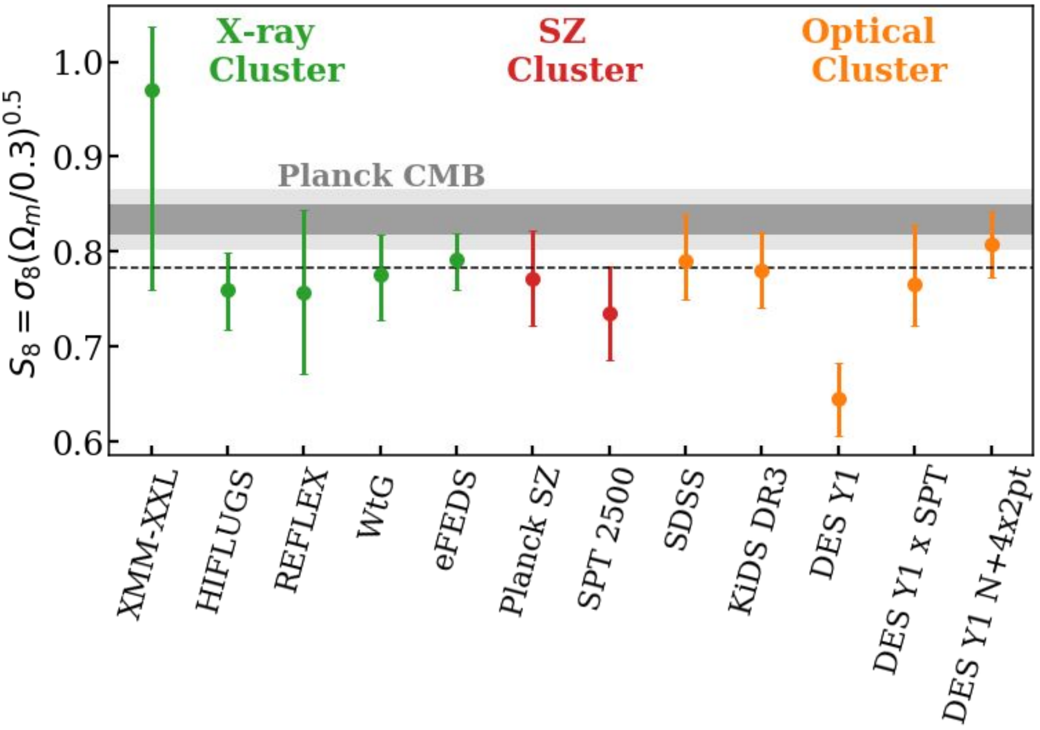

DES Collaboration 2020

- Cosmological constraints independent and competitive with other cosmological probes
- Slight to moderate tension between different cluster studies
- Currently limited by the mass (i.e. scaling relation) calibration

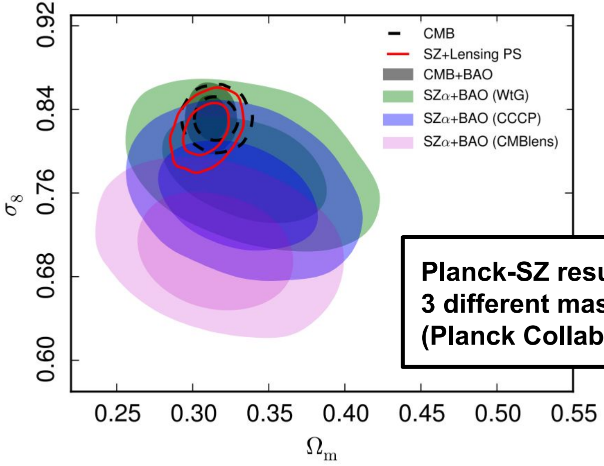

Planck-SZ results assuming 3 different mass calibrations (Planck Collaboration 2015)

RECENT CONSTRAINTS FROM CLUSTER NC

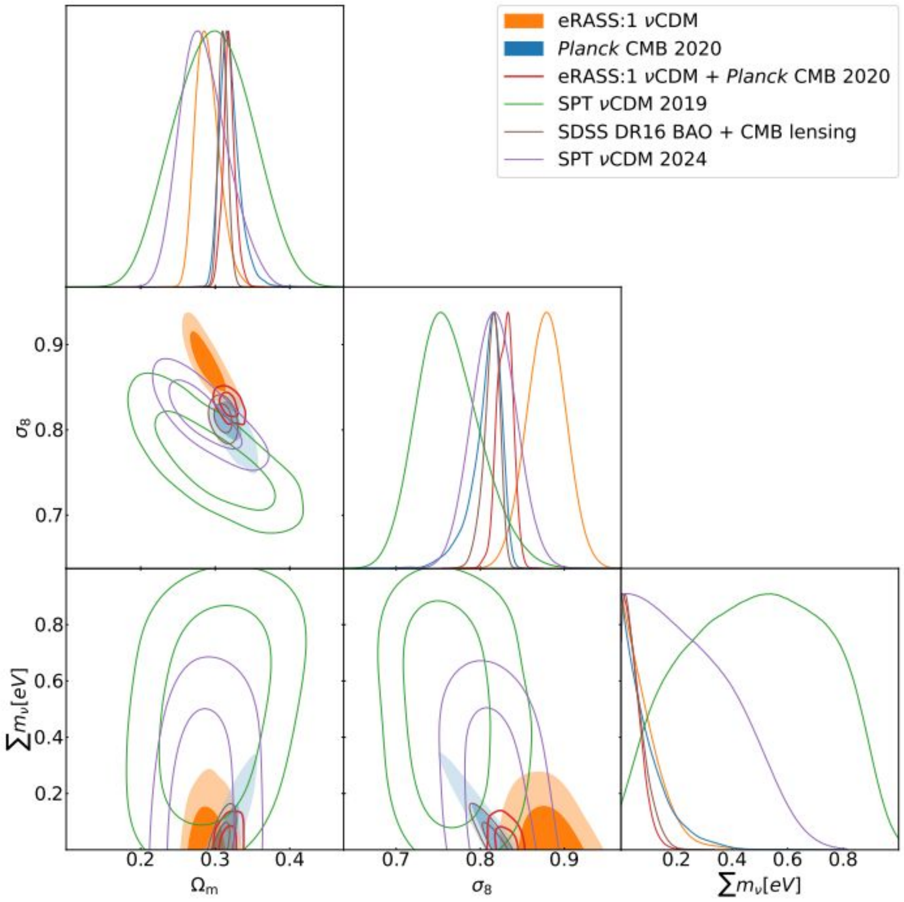

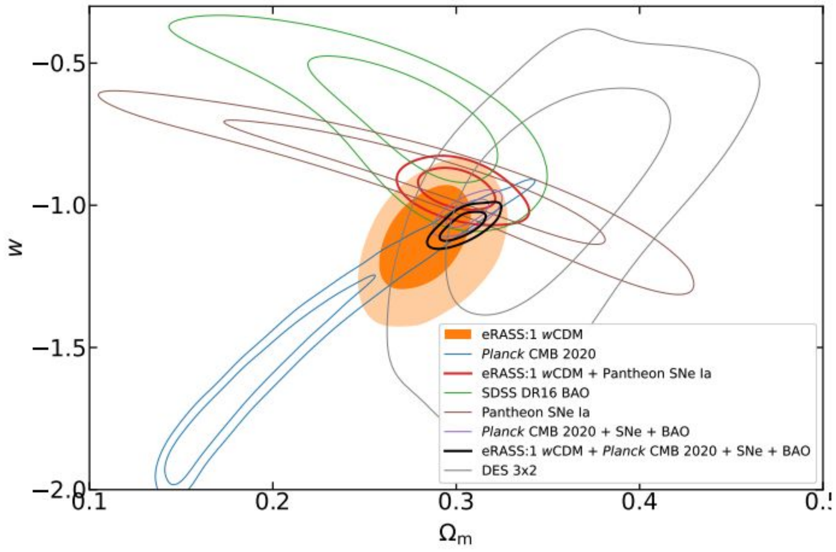

https://arxiv.org/pdf/2402.08458.pdf

OTHER COSMOLOGICAL TESTS WITH GALAXY CLUSTERS

OTHER COSMOLOGICAL TESTS WITH GALAXY CLUSTERS

- **The Bullet Cluster (DM nature)**

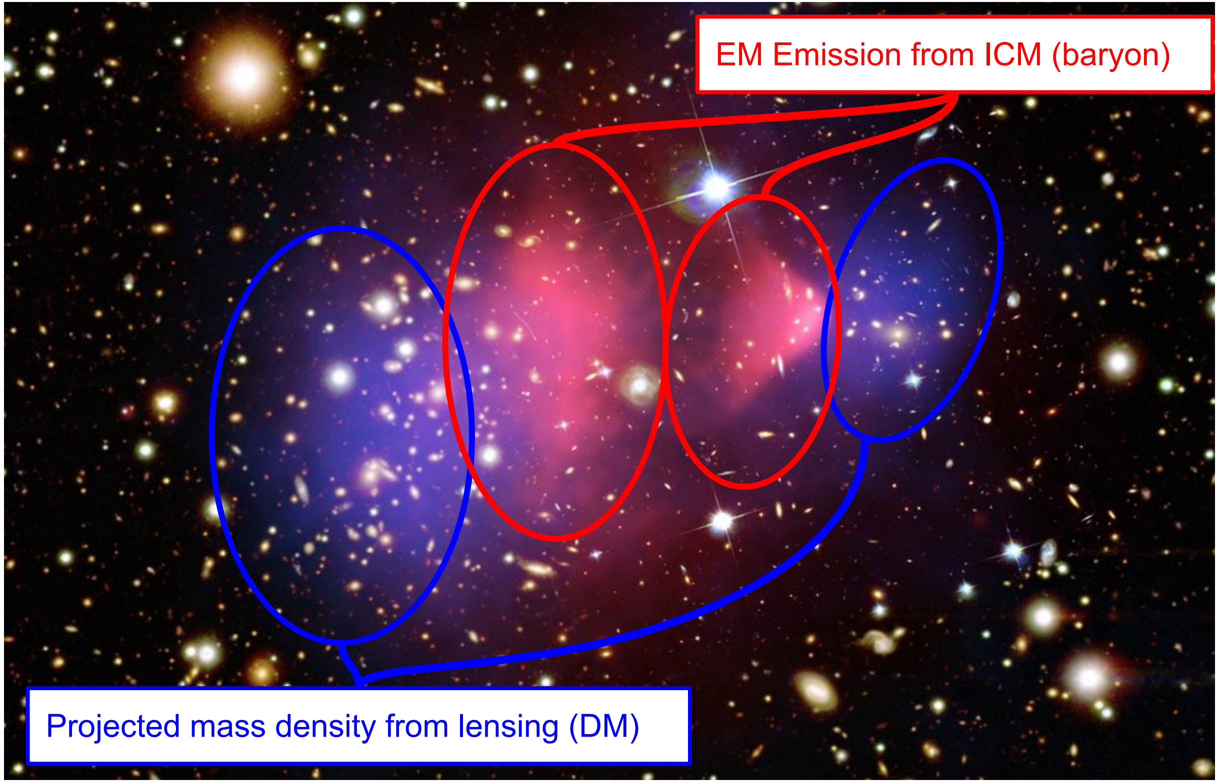

Real vs simulated Bullet-like shock (Keshet+21)

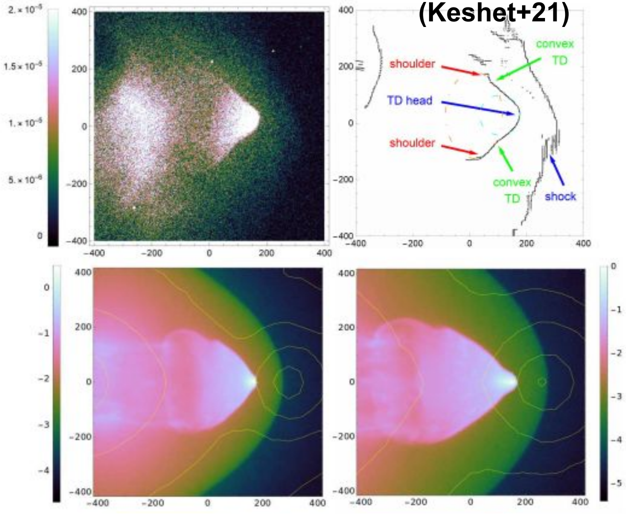

The offset between the EM and WL signal peaks, along with the shape of the shock wave, provide compelling evidence for the presence of dark matter; moreover it allows to place constraints on the dark matter cross-section

OTHER COSMOLOGICAL TESTS WITH GALAXY CLUSTERS

Mass estimates from accretion shocks https://arxiv.org/abs/2407.01660: Utilizing a sample of simulated galaxy clusters the analysis reveals that these clusters lie on a well-defined plane within the three-dimensional space defined by mass (M), shock radius (R_s), and Mach number $\mathscr{M}$ (indicating shock strength). This planar relationship suggests a predictable correlation among these parameters.

$$\log_{10}\frac{M(<2R_{\rm vir})}{M_\odot} = 12.760 + 1.910\log_{10}\frac{R_{\rm sh}}{\rm Mpc} + 0.0117\mathscr{M}_{\rm sh}, \qquad (\text{at } z=0)$$

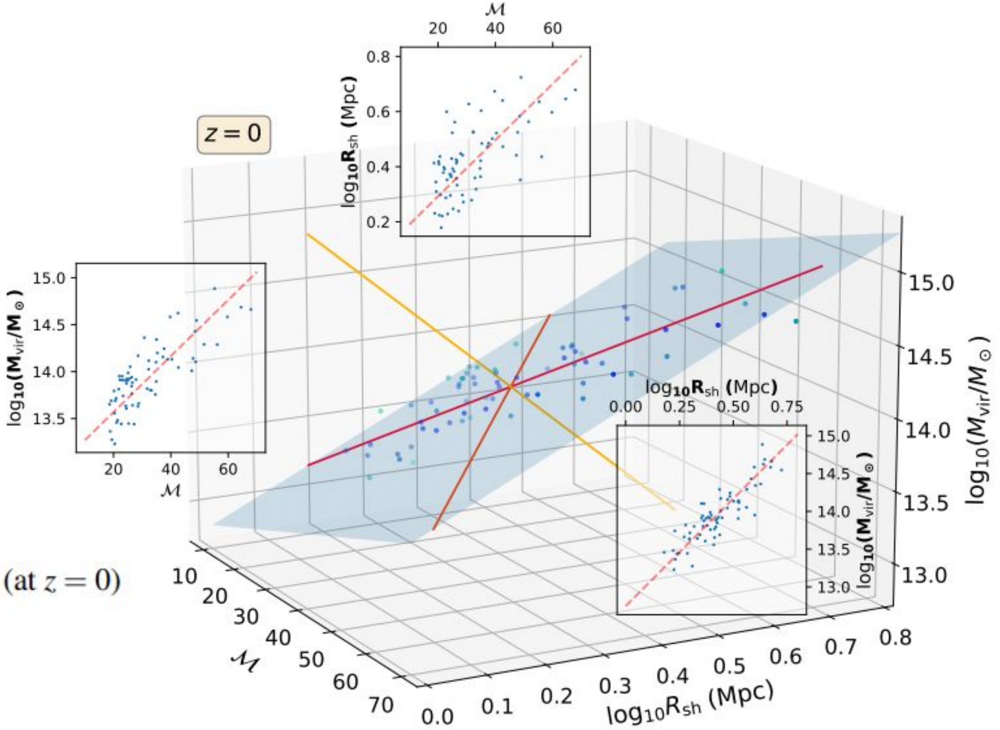

OTHER COSMOLOGICAL TESTS WITH GALAXY CLUSTERS

- **Gas mass fraction (Ω_m,Ω_Λ, w):**

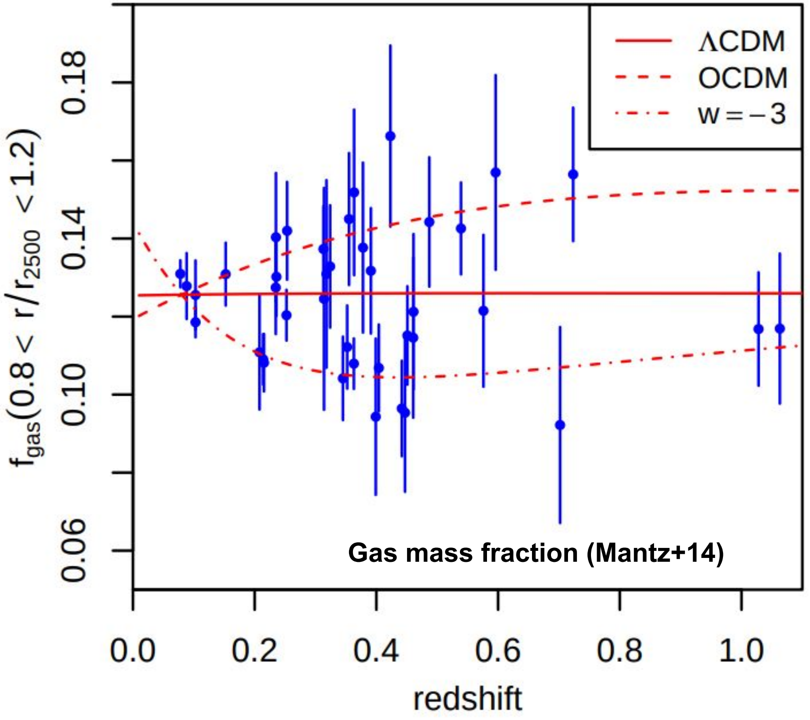

$$f_{\rm gas} = \frac{M_{\rm gas}}{M_{\rm tot}} \propto \left(\frac{\Omega_b}{\Omega_m}\right) \left[\frac{d^{\rm ref}(z)}{d(z)}\right]^{3/2}$$

With priors on

1. $\Omega_{\rm b} h^2$ (important)
2. h (less important),

the low-z data constrain $\Omega_{\rm m}$:

$$f_{\rm gas}(z \lesssim 0.15) \propto \frac{\Omega_{\rm b}}{\Omega_{\rm m}} h^{3/2}$$

Apparent evolution constrains dark energy:

$$f_{\rm gas}(z) \propto d(z)^{-3/2}$$

Credit A. Mantz

OTHER COSMOLOGICAL TESTS WITH GALAXY CLUSTERS

H_0 from X-ray and SZ distance measurements:

Based on a distance measuring techniques that depend on a comparison of 2 observables (Cavaliere+77):

$$E \propto \int n_e^2 dl$$

$$A \propto \int n_e dl$$

If the structure of the gas is known, given the angular size ϑ of the system, the angular diameter distance is given by:

$$D_A(z) = A^2/(E\theta)$$

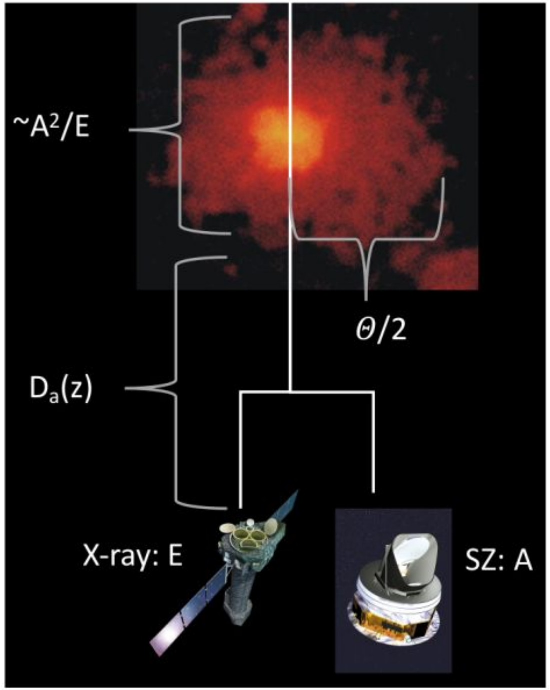

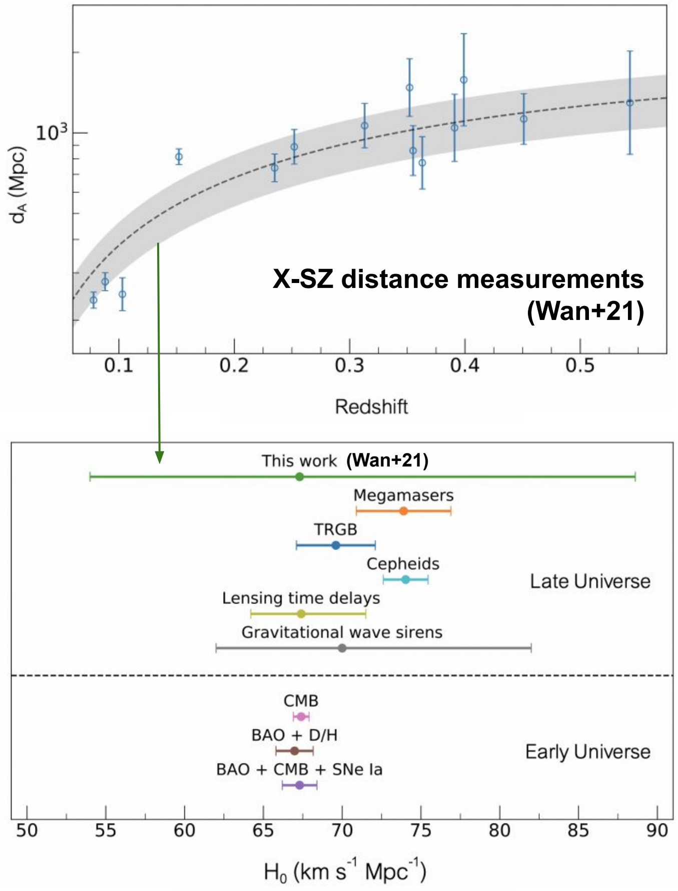

THE HALO PROFILE

From n-body/hydro simulations we can predict the dark matter/gas (spherically averaged) halo profiles. For LCDM models E.g. Navarro+97 and Einasto 1965:

$$\rho_{\rm NFW} = \frac{\rho_{\rm s}}{(r/r_{\rm s})(1+r/r_{\rm s})^2}$$

$$\rho_{\rm Ein} = \rho_{-2}\exp\left\{-\frac{2}{\alpha}\left[\left(\frac{r}{r_{-2}}\right)^{\alpha}-1\right]\right\}$$

Observationally, cluster profiles can be inferred from strong and weak lensing, galaxy dynamics, and ICM (X-ray,SZ) measurements

DM halo profiles for halos of different mass and redshift

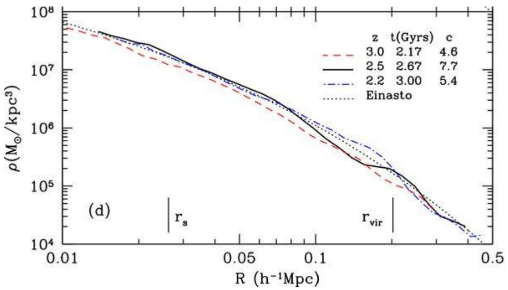

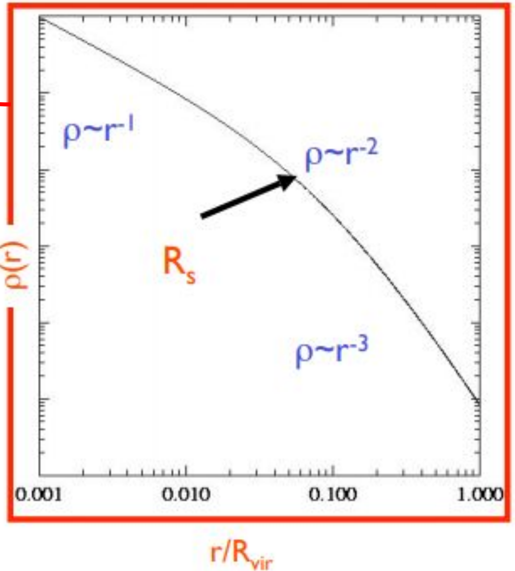

$c_{\rm NFW} = r_{200}/r_s$

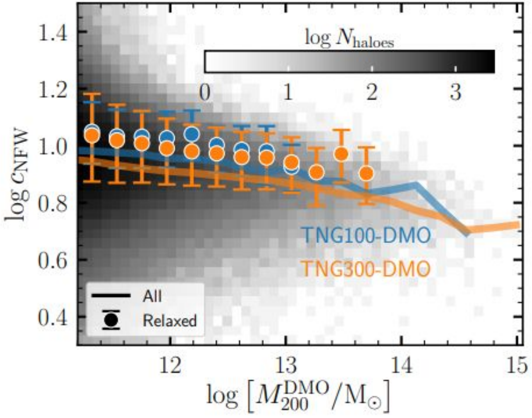

Concentration-mass relation in TNG simulation (Bose+19)

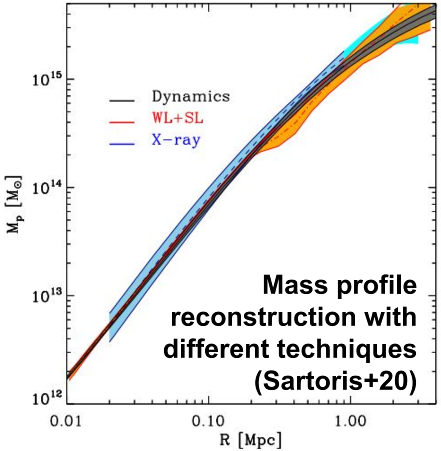

Mass profile reconstruction with different techniques (Sartoris+20)

OTHER COSMOLOGICAL TESTS WITH GALAXY CLUSTERS

- **Galaxy cluster mass profile:**

The shape/slope of the halo profile, especially in the inner regions, can be used to test several fundamental physics model, such as the nature of dark matter (e.g. warm vs cold, interacting DM) or GR test.

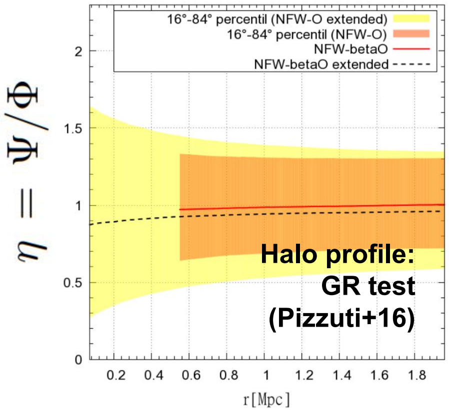

Halo profile: GR test (Pizzuti+16)

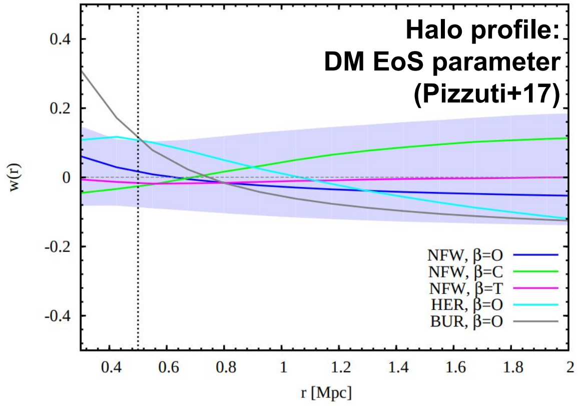

Halo profile: DM EoS parameter (Pizzuti+17)

Halo profile: Interacting DM vs DM (Vega-Ferrero+20)

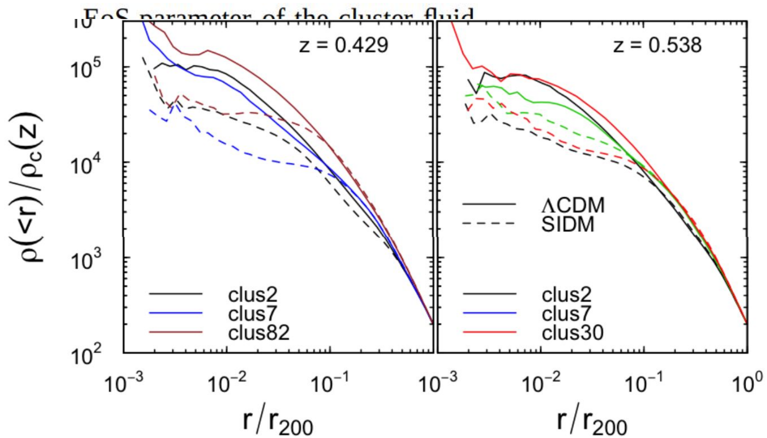

Halo profile: f(R) constraints (Butt+25)

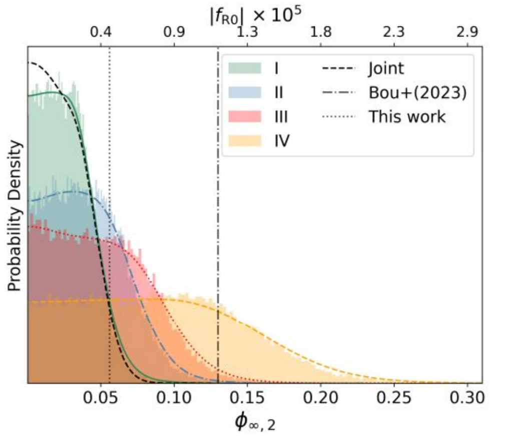

STATISTICAL PROPERTIES OF THE LARGE SCALE STRUCTURES:

CLUSTERING

For a review on structure formation:
https://sites.astro.caltech.edu/~george/ay127/kamionkowski-perturbations-notes.pdf
https://people.ast.cam.ac.uk/~pettini/Intro%20Cosmology/Lecture14.pdf
For a review on BAO: https://arxiv.org/pdf/0910.5224.pdf
For a review on RSD: https://arxiv.org/pdf/astro-ph/9708102.pdf

EVOLUTION OF DENSITY PERTURBATIONS

Inflation generates primordial perturbations through the amplification of quantum fluctuations, which are stretched to astrophysical scales by the rapid expansion.

The simplest models of inflation predict that the initial fluctuations constitute a Gaussian random field, with an almost purely adiabatic primordial perturbations with a near scale-invariant power spectrum. In these models the primordial power spectrum is often described in terms of a spectral index n_s and an amplitude of the perturbations A_s as (k_p = 0.05 Mpc^{-1} = pivot scale):

$$P(k) = A_s \left(\frac{k}{k_p}\right)^{n_s}$$

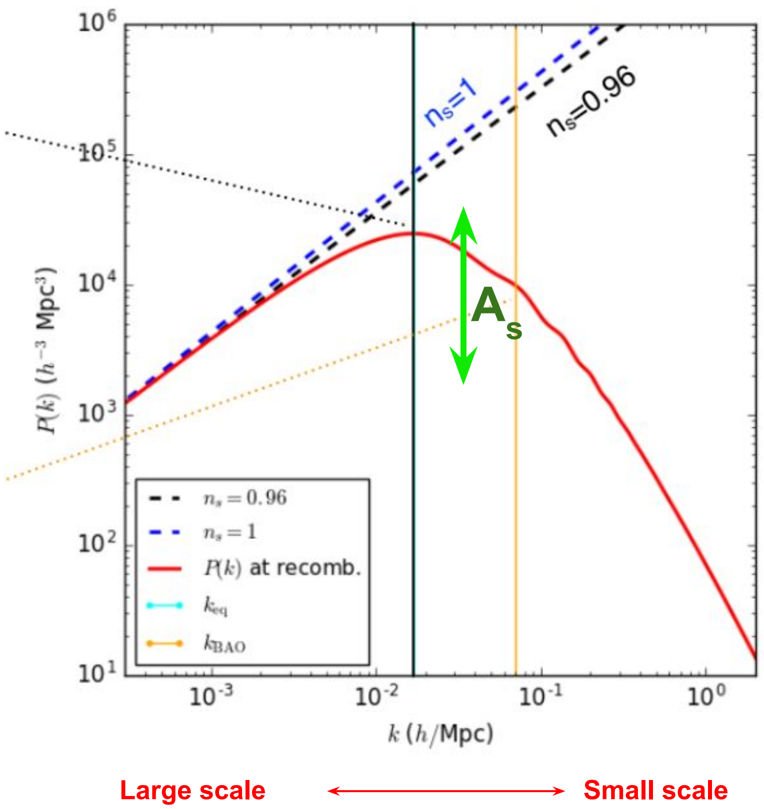

EVOLUTION OF DENSITY PERTURBATIONS

After the perturbations are created in the early Universe, they undergo a complex evolution which depends on the theory of gravity (GR), and the expansion history of the Universe.

- **Gravity is the dominant force that moves matter on the largest scales.**
- **The dark matter, which constitutes ~ 5/6 of the nonrelativistic matter in the Universe, is composed of "cold dark matter", pressureless matter that interacts with everything else only gravitationally.**

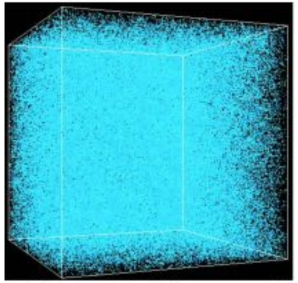
Universe 120 million years old

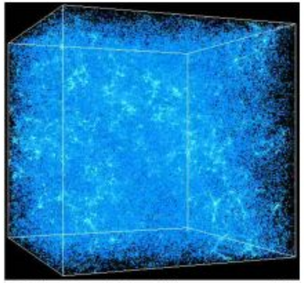
Universe 490 million years old

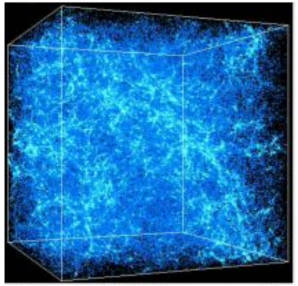
Universe 1.2 billion years old

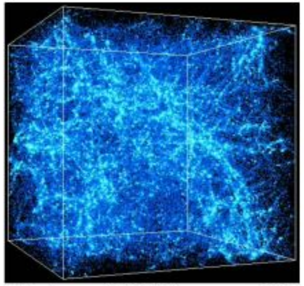
Universe 2.2 billion years old

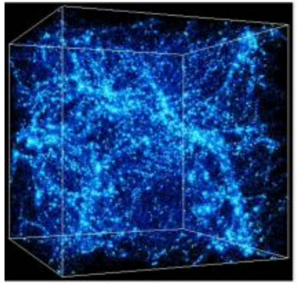
Universe 6.0 billion years old

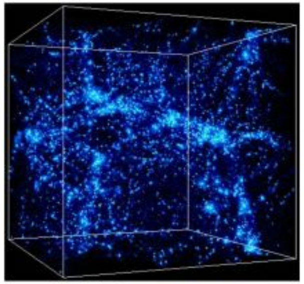
Universe 13.7 billion years old

EVOLUTION OF DENSITY PERTURBATIONS

- **Overdensity field:**

$$\delta(\mathbf{x}) \equiv \frac{\rho(\mathbf{x}) - \langle\rho\rangle}{\langle\rho\rangle}$$

For CDM model:

	$z > z_{eq}$ **(RD)**	$z < z_{eq}$ **(MD)**
$R > R_H$	$\delta_r \propto \delta_m \propto a^2$	$\delta_r \propto \delta_m \propto a$
$R < R_H$	$\delta_{cdm} \sim const$ $\delta_{b+\gamma}\ oscillations$	$\delta_{cdm} \propto a$ $z < z_{rec}:\ \delta_b \rightarrow \delta_{cdm}$

Matter-radiation equality

$$\frac{\rho_m(a_{eq})}{\rho_r(a_{eq})} = 1$$

$$1 + z_{eq} = \frac{a_0}{a_{eq}} \simeq 3250$$

Hubble radius

$$R_H(t) = \frac{c}{H(t)} \sim c\,t$$

EVOLUTION OF DENSITY PERTURBATIONS

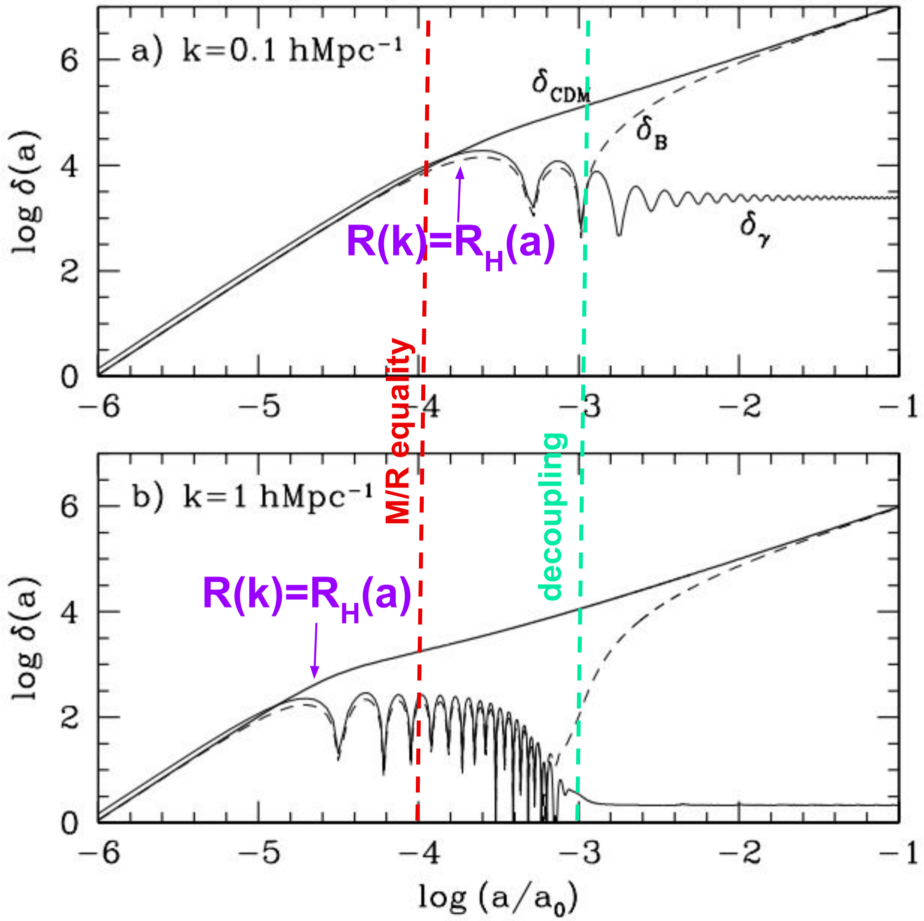

The evolution of adiabatic perturbations in a CDM universe with $\Omega_{m,0} = 1$, $\Omega_{B,0} = 0.05$, $h = 0.5$.
The scale factor is normalized at the present time.
Decoupling: $a \sim 10^{-3}$
Matter/radiation equality: $a \sim 10^{4}$

Note: Since these modes enters horizon after (k=0.1) or just before (k=1) matter-radiation equality, there is no Meszaros effect (δ_{cdm} ~ cost)

EVOLUTION OF DENSITY PERTURBATIONS

The primordial power spectrum of density fluctuations gets "processed" by the growth of density perturbations:

$$P(k, z) = P_{\rm primordial}(k)T^2(k, z)$$

where the transfer function T(k) takes into account the effects of gravitational amplification of density perturbation mode of wavelength *k*

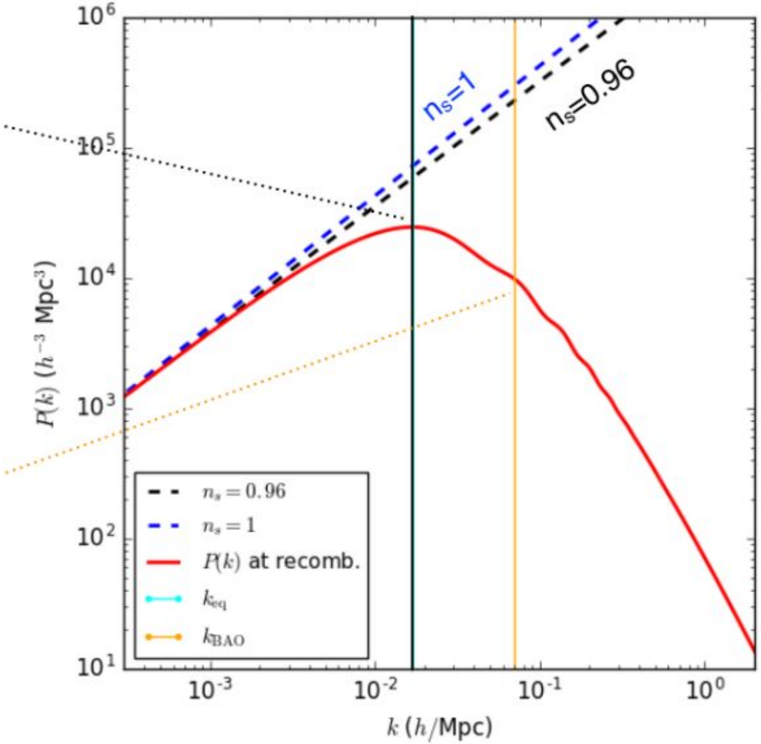

EVOLUTION OF DENSITY PERTURBATIONS

The primordial power spectrum of density fluctuations gets "processed" by the growth of density perturbations:

$$P(k, z) = P_{\mathrm{primordial}}(k) T^2(k, z)$$

where the transfer function T(k) takes into account the effects of gravitational amplification of density perturbation mode of wavelength *k*

Transfer function for different components

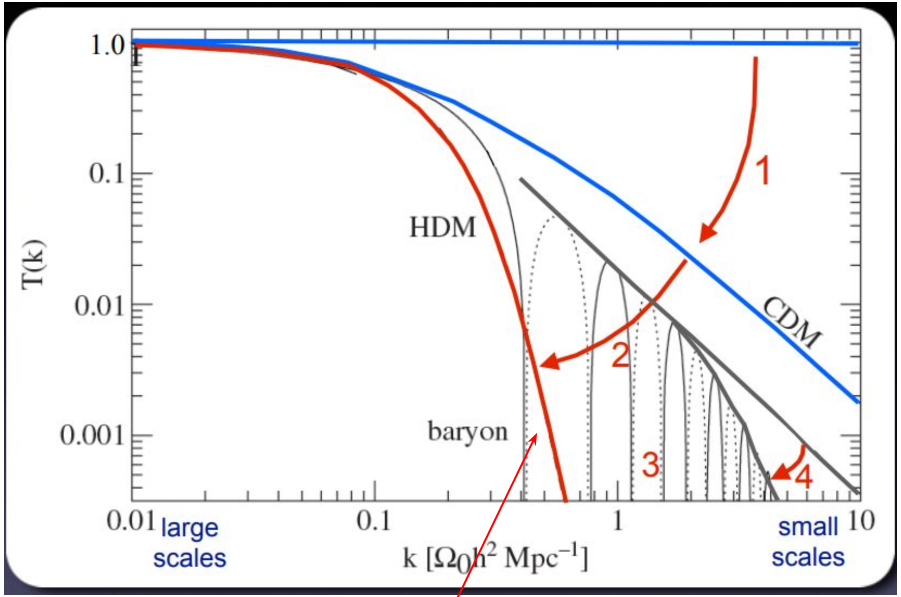

Note: The thermal velocity of DM particles determines the free streaming length below which structure formation is suppressed (free-streaming damping)

SIDE NOTE: HOT, WARM AND COLD DARK MATTER

Free-streaming cut-off scale:

$$k_{\rm FS} \sim 15.6 \frac{h}{\rm Mpc} \left(\frac{m_{\rm WDM}}{1 \rm keV}\right)^{4/3} \left(\frac{0.12}{\Omega_{DM} h^2}\right)^{1/3}$$

Cosmic Relics

Non-thermal Relics

not produced in thermal equilibrium (TE) with rest of Universe.

e.g., axions (FDM), monopoles, cosmic strings

Thermal Relics

are held in TE with other components of Universe until they `decouple', which happens when interaction rate $\Gamma = n\langle\sigma v\rangle$ drops below expansion rate $H(a)$

Hot Dark Matter

particles are still relativistic at decoupling, i.e., $3k_{\rm B}T_{\rm d} > m_{\rm X}c^2$

e.g., massive neutrinos

Cold Dark Matter

particles are non-relativistic at decoupling i.e., $3k_{\rm B}T_{\rm d} < m_{\rm X}c^2$

e.g., WIMPS

Warm Dark Matter

E.g. keV sterile neutrino

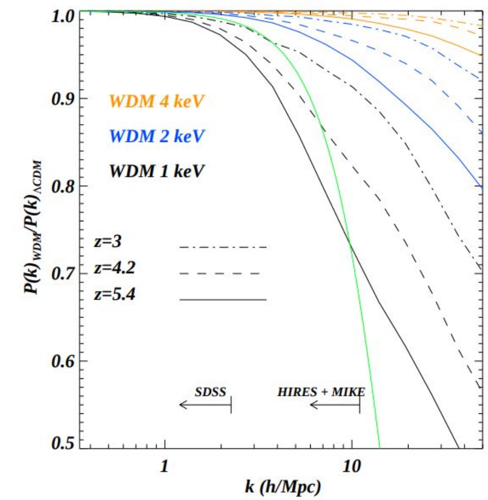

EVOLUTION OF DENSITY PERTURBATIONS

Transfer function (CDM):

$$T(k) \simeq \begin{cases} 1, & k \lesssim k_{\rm eq}, \\ (k/k_{\rm eq})^{-2}, & k \gtrsim k_{\rm eq}, \end{cases}$$

The characteristic length scale is the horizon-size at matter-radiation equality, $k_{eq} = 2\pi(ct_{eq})^{-1} \propto \Omega_{m,0}h^2$: before t_{eq}, below the horizon, dark matter fluctuations cannot growth.

Thus, if $P_{primordial}(k) \propto k^n$, the processed power spectrum is:

- **$P(k) \propto k^n$ for $k \ll k_{eq}$ (above the horizon)**
- **$P(k) \propto k^{n-4}$ for $k \gg keq$ (below the horizon)**

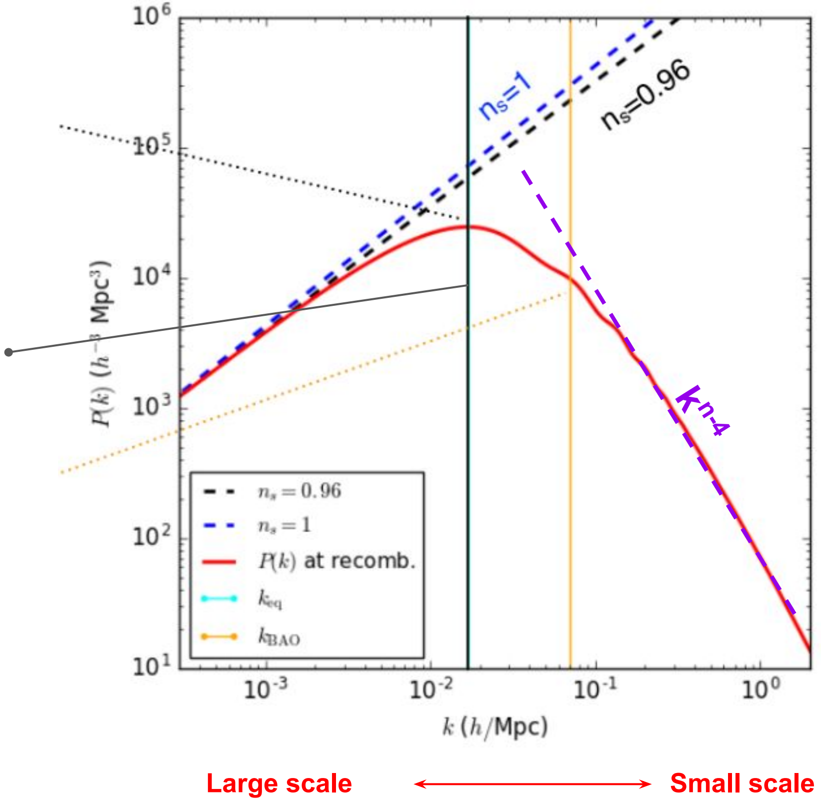

EVOLUTION OF DENSITY PERTURBATIONS

Baryonic Acoustic Oscillations:

In the early, high-temperature Universe, baryons and photons were tightly coupled by Compton scattering, in a so-called photon-baryon fluid; the competing forces of radiation pressure and gravity set up oscillations in the photon-baryon fluid. As the Universe expands and cools down, atoms form (Recombination) and the interaction rate between baryons and photons decreases: photons begin to free-stream, leaving baryons in a shell with a radius approximately equal to the sound horizon at the time of decoupling. From that moment on, only the gravitational interaction between dark matter and baryonic matter remains. This characteristic radius is therefore imprinted as an overdensity and the power spectrum have an excess of power on this scale.